Inorganic Chemistry
Article

Inorg. Chem. **2009**, *48*, 11847–11852 **11847**
DOI: 10.1021/ic9018647

Evidence of Disruption of Conjugation Involving Delta Bonds in Intramolecular Electronic Coupling

F. Albert Cotton,† Zhong Li, and Carlos A. Murillo*

Department of Chemistry, Laboratory for Molecular Structure and Bonding, P.O. Box 30012, Texas A&M University, College Station, Texas 77842-3012. † Deceased, February 20, 2007.

Received September 21, 2009

A *dimer of dimers* containing two quadruply bonded $[Mo_2(DAniF)_3]^+$ units (DAniF = *N,N′*-di(*p*-anisyl)formamidinate) linked by the S-donor linker, dimethyldithiooxamidate was synthesized, structurally characterized, and electronic communication was probed. The core of $[Mo_2(DAniF)_3]_2(C_2S_2N_2Me_2)$, **1**, formed by the $Mo_2NSC_2SNMo_2$ atoms shows two fused but non planar six-membered rings, which differs from that of the β form of dimethyloxamidate analogue that has a heteronaphthalene-type structure (Cotton, F. A.; Liu, C. Y.; Murillo, C. A.; Villagrán, D.; Wang, X. *J. Am. Chem. Soc.* **2004**, *126*, 14822). For these two analogous compounds electronic coupling between the two $[Mo_2]$ units, as determined by electrochemical measurements, diminishes considerably upon replacement of O-donor by S-donor atoms ($\Delta E_{1/2}$ = 531 mV and 440 mV, respectively). This suggests that the non planar conformation of the linker in **1** hampers a pathway leading to π conjugation. Density functional theory (DFT) calculations show that the highest occupied molecular orbitals HOMO−HOMO-1 energy gap of 0.12 eV for **1** is much smaller than that of 0.61 eV for the O-donor analogue, which is consistent with the electrochemical data.

Introduction

Electron transfer is a ubiquitous process of enormous importance not only in chemistry but also in many other fields such as molecular electronics, photosynthesis, and biosensors.[1] Since the late 1960s when the Creutz−Taube (CT) ion was synthesized, compounds with two or more identical redox centers joined by a linker have been of great interest[2] for modeling intramolecular electronic coupling and the design of new materials.[3] Experimental and theoretical studies on these systems have been essential in providing a better understanding of electron transfer processes.

Many techniques employing electrochemical, spectroscopic, and magnetic measurements have been used to evaluate electronic communication between metal units and the effect of the linker. In general, electrochemical measurements of these compounds show two successive one-electron redox processes, and the separation between the two $E_{1/2}$ values, $\Delta E_{1/2}$, is associated with the comproportionation constant K_C.[4]

$$M^n \sim M^n + M^{(n+l)+} \sim M^{(n+l)+} \rightleftharpoons 2[M \sim M]^{(2n+l)+} \quad K_C$$

The free energy of comproportionation, ΔG_C, is calculated using the thermodynamic relationship $\Delta G_C = -RT \ln(K_C)$. The value of ΔG_C may be viewed as being affected by a series of contributing factors,[5] such as those in the commonly used expression:[6]

$$\Delta G_C = \Delta G_S + \Delta G_E + \Delta G_R + \Delta G_I$$

where ΔG_S is a small statistical contribution to the comproportionation equilibrium, ΔG_E accounts for the electrostatic

*To whom correspondence should be addressed. E-mail: murillo@tamu.edu.

(1) See for example: (a) Brunschwig, B. S.; Sutin, N. *Coord. Chem. Rev.* **1999**, *187*, 233. (b) Holm, R. H.; Kennepohl, P.; Solomon, E. I. *Chem. Rev.* **1996**, *96*, 2239. (c) Marcus, R. A. *J. Electroanal. Chem.* **1997**, *438*, 251. (d) Cameron, C. G.; Pickup, P. G. *J. Am. Chem. Soc.* **1999**, *121*, 7710. (e) Demadis, K. D.; Hartshorn, C. M.; Meyer, T. J. *Chem. Rev.* **2001**, *101*, 2655. (f) Lau, V. C.; Berben, L. A.; Long, J. R. *J. Am. Chem. Soc.* **2002**, *124*, 9042. (g) Shi, Y.; Yee, G. T.; Wang, G.; Ren, T. *J. Am. Chem. Soc.* **2004**, *126*, 10552.

(2) Kaim, W.; Klein, A.; Glockle, M. *Acc. Chem. Res.* **2000**, *33*, 755.

(3) See for example: (a) *Mixed-valency Systems: Applications in Chemistry, Physics and Biology*; Prassides, K., Ed.; Kluwer Academic Publishers: Dordrecht, 1991. (b) Cembran, A.; Bernardi, F.; Olivucci, M.; Garavelli, M. *Proc. Natl. Acad. Sci. U.S.A.* **2005**, *102*, 6255. (c) Talukdar, P.; Bollot, G.; Mareda, J.; Sakai, N.; Matile, S. *J. Am. Chem. Soc.* **2005**, *127*, 6528. (d) Fiedler, A. T.; Bryngelson, P. A.; Maroney, M. J.; Brunold, T. C. *J. Am. Chem. Soc.* **2005**, *127*, 5449. (e) Sakharov, D. V.; Lim, C *J. Am. Chem. Soc.* **2005**, *127*, 4921. (f) Efimov, I.; McIntire, W. S. *J. Am. Chem. Soc.* **2005**, *127*, 732. (g) O'Neill, M. A.; Dohno, C.; Barton, J. K. *J. Am. Chem. Soc.* **2004**, *126*, 1316. (h) Lewis, F. D.; Wu, Y.; Zhang, L.; Zuo, X.; Gayes, R. T.; Wasielewski, M. R. *J. Am. Chem. Soc.* **2004**, *126*, 8206. (i) Wan, C.; Fiebig, T.; Schiemann, O.; Barton, J. K.; Zewail, A. H. *Proc. Natl. Acad. Sci. U.S.A.* **2000**, *97*, 14052. (j) Hess, S.; Götz, M.; Davis, W. B.; Michel-Beyerle, M. E. *J. Am. Chem. Soc.* **2001**, *123*, 10046.

(4) Richardson, D. E.; Taube, H. *Coord. Chem. Rev.* **1984**, *60*, 107.

(5) See for example: (a) DeRosa, M. C.; White, C.; Evans, C. E. B.; Crutley, R. J. *J. Am. Chem. Soc.* **2001**, *123*, 1396. (b) Chen, Y. J.; Pan, D.-S.; Chiu, C.-F.; Su, J.-X.; Lin, S. J.; Kwan, S. K. *Inorg. Chem.* **2000**, *39*, 953.

(6) Evans, C. E. B.; Naklicki, M. L.; Rezvani, A. R.; White, C. A.; Kondratiev, V. V.; Crutchley, R. J. *J. Am. Chem. Soc.* **1998**, *120*, 13096.

Published on Web 11/13/2009

Scheme 1

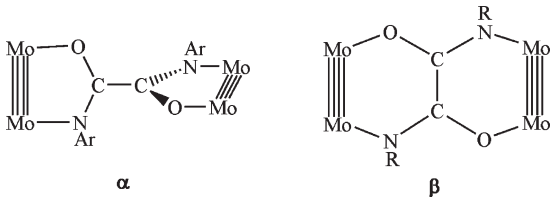

repulsion of the metal centers, ΔG_R is the free energy of resonance exchange or electron delocalization, and ΔG_I is a contribution from inductive factors. Values of K_C obtained under similar experimental conditions for closely related systems have often been used for comparing electronic coupling between metal centers through a linker.

Recently, analogues containing two dimetal species, usually quadruple bonded Mo_2^{4+} units, linked by a variety of bridging ligands with a general formula $[M_2]L[M_2]$ (where $[Mo_2]$ = a unit such as $Mo_2(DAniF)_3$ or $Mo_2(cis\text{-}DAniF)_2$ and DAniF = *N*,*N*′-di-*p*-anisylformamidinate) have been very useful in evaluating electronic communication between dimetal units because they provide new probes unavailable for compounds containing single metal units such as the CT species.[7] In early work, dianions of dicarboxylic acids were the most frequently employed linkers, but they were generally marginal in mediating electronic communication.[8] However, by replacing half of O-donor atoms from dicarboxylate linkers by N-donor atoms, the corresponding diamidate ligands significantly increased electronic coupling.[9] In addition such compounds had some useful properties since the latter are quite stable because the ligands are much stronger Lewis bases than the carboxylate groups. Furthermore substituents on the nitrogen atoms may be synthetically adjusted both sterically and electronically.[9] Interestingly, when either of the diaryloxamidate $[ArNC(O)C(O)NAr]^{2-}$ (Ar = phenyl or *p*-anisyl) groups serve as linkers, two geometric isomers can be isolated depending on the reaction conditions.[10] The two isomers, designated as α and β (Scheme 1), entail different binding modes of the diaryloxamidate ligand. The electronic coupling between two $[Mo_2]$ units in these two molecules is quite different as measured from the separation of oxidation potentials ($\Delta E_{1/2}$). For the α isomer $\Delta E_{1/2}$ is about 190 mV but increases to about 530 mV for the β form. In the α form, the orbital interaction between two dimetal units is negligible but in the β form π conjugation, resembling that in naphthalene, exists. This has led to the suggestion that in these dimolybdenum compounds electrons in the δ orbitals of the Mo_2 units are involved in conjugation.

Lately there has been interest in linkers with sulfur donor atoms since such donor atoms are important in modifying electron transfer processes and are useful in enzyme reactivity.[11] The Chisholm group reported improvement of electronic coupling for *dimers of dimers* by stepwise replacement of O to S from dicarboxylates.[12] More recently, when the O-donor atoms in oxamidate were replaced by S-donor atoms, coupling in these dithiooxamidate species was greatly enhanced because of dδ-dπ interactions between the dimetal units and the low-lying π* orbital of the sulfur atoms.[13] Such interactions led to low energy metal-to-ligand charge transfer processes which facilitate electron-hopping pathways.

We also showed that in tetranuclear clusters of the type $[Mo_2]_2(\mu\text{-E—E})_2$ (where E—E represents a bidentate ligand with donor atoms E = O or S) the electronic coupling for compounds with E = S is substantially stronger than for those with E = O.[14] For this type of compounds with two linkers joining the dimetal units, density functional theory (DFT) calculations suggest that the highest occupied molecular orbital (HOMO) is primarily a metal-based orbital and there are no low-lying π* orbitals in the ligand sulfur atoms.[14] A major difference between the electronic structure of oxygen and the electronic structure of sulfur atoms is that empty d orbitals are available for sulfur, and this element tends to form links with multiple bond character.[15] This is evidenced by the relative bond energies of the E−O single bonds which are stronger for S−O than for O−O bonds. However, for E = O double bonds, the S═O bond is weaker than the O═O double bond, because the larger radius of the sulfur atom leads to reduced overlap for σ and π interactions relative to the bonds with oxygen atoms.

For the *dimers of dimers* without a π system the electronic coupling is usually weak, as found for example in the α form of the oxamidate analogues.[10] In such compounds with an α-type arrangement (Scheme 1), the electronic coupling is enhanced by replacing oxygen to sulfur atoms because the latter introduce some π bonding character as observed in dithiooxamidate-linked compound.[13]

Here we examine what happens when an oxygen atom is replaced by a sulfur atom in a system analogous to that containing the β oxamidate form, which is known to provide a high degree of π conjugation and shows strong electronic coupling, and report the synthesis of a dimolybdenum pair linked by dimethyldithiooxamidate, $[Mo_2(DAniF)_3]_2(C_2S_2N_2Me_2)$. A significant reduction in the electronic coupling between the two $[Mo_2(DAniF)_3]$ units compared to that of dimethyloxamidate-linked analogue[16] was observed.

Results and Discussion

The synthesis of $[Mo_2(DAniF)_3]_2(C_2S_2N_2Me_2)$, **1**, was carried out by reacting the mixed-ligand precursor $Mo_2(DAniF)_3(O_2CCH_3)$[10a] and *N*,*N*′-dimethyldithiooxamide as

(7) (a) Cotton, F. A.; Lin, C.; Murillo, C. A. *Acc. Chem. Res.* **2001**, *34*, 759. (b) Cotton, F. A.; Lin, C.; Murillo, C. A. *Proc. Natl. Acad. Sci. U.S.A.* **2002**, *99*, 4810. (c) Chisholm, M. H.; Macintosh, A. M. *Chem. Rev.* **2005**, *105*, 2929. (d) Chisholm, M. H. *Proc. Natl. Acad. Sci. U.S.A.* **2007**, *104*, 2563. (e) Chisholm, M. H.; Patmore, N. J. *Acc. Chem. Res.* **2007**, *40*, 19.

(8) (a) Cotton, F. A.; Donahue, J. P.; Lin, C.; Murillo, C. A. *Inorg. Chem.* **2001**, *40*, 1234. (b) Cotton, F. A.; Donahue, J. P.; Murillo, C. A. *J. Am. Chem. Soc.* **2003**, *125*, 5436. (c) Cotton, F. A.; Donahue, J. P.; Murillo, C. A.; Pérez, L. M. *J. Am. Chem. Soc.* **2003**, *125*, 5486.

(9) Cotton, F. A.; Li, Z.; Liu, C. Y.; Murillo, C. A. *Inorg. Chem.* **2006**, *45*, 9765.

(10) (a) Cotton, F. A.; Liu, C. Y.; Murillo, C. A.; Villagrán, D.; Wang, X. *J. Am. Chem. Soc.* **2003**, *125*, 13564. (b) Cotton, F. A.; Liu, C. Y.; Murillo, C. A.; Zhao, Q. *Inorg. Chem.* **2007**, *46*, 2604.

(11) (a) Hille, R. *Chem. Rev.* **1996**, *96*, 2757. (b) Czjzek, M.; Santos, J.-P. D.; Pomier, J.; Giordano, G.; Méjean, V.; Haser, R. *J. Mol. Biol.* **1998**, *284*, 435. (c) Hânzelmann, P.; Schindelin, H. *Proc. Natl. Acad. Sci. U. S. A.* **2004**, *101*, 12870. (c) Brondino, C. D.; Rivas, M. G.; Romao, M. J.; Moura, J. J. G.; Moura, I. *Acc. Chem. Res.* **2006**, *39*, 788.

(12) Chisholm, M. H.; Patmore, N. J. *Dalton Trans.* **2006**, 3164.

(13) Cotton, F. A.; Li, Z.; Liu, C. Y.; Murillo, C. A. *Inorg. Chem.* **2007**, *46*, 7840.

(14) Cotton, F. A.; Li, Z.; Liu, C. Y.; Murillo, C. A. *Inorg. Chem.* **2007**, *46*, 9294.

(15) Cotton, F. A.; Wilkinson, G.; Murillo, C. A.; Bochmann, M. *Advanced Inorganic Chemistry*, 6th ed.; John Wiley & Sons, Inc: New York, 1999.

(16) Cotton, F. A.; Liu, C. Y.; Murillo, C. A.; Villagrán, D.; Wang, X. *J. Am. Chem. Soc.* **2004**, *126*, 14822.

Scheme 2

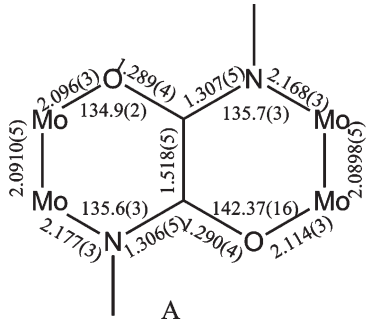

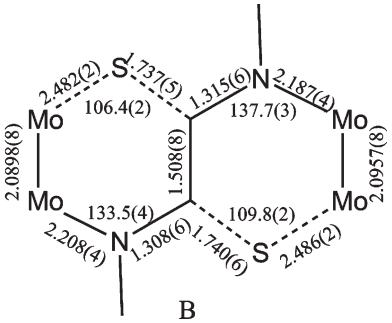

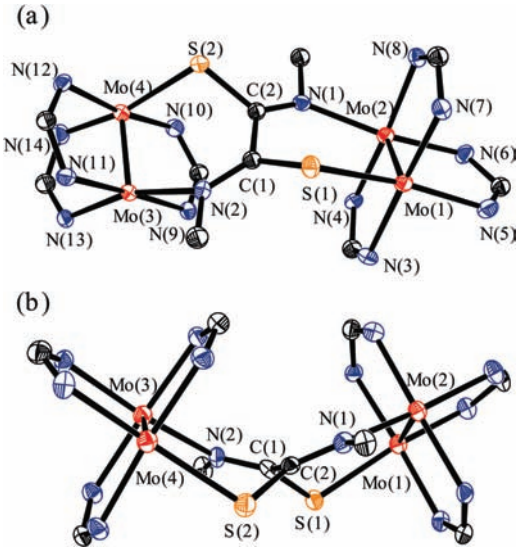

Figure 1. Two different views of the core structure of **1** with displacement ellipsoids drawn at the 40% probability level. The bottom view clearly shows a butterfly arrangement. All *p*−anisyl groups and hydrogen atoms have been omitted for clarity.

Table 1. Selected Bond Lengths (Å) and Angles (deg) for **1**·2CH_2Cl_2 and Geometric Parameters from DFT Calculations for the Model of **1**

	1·1.5CH_2Cl_2	calculated
Mo(1)−Mo(2)	2.0957(8)	2.1423
Mo(3)−Mo(4)	2.0898(8)	2.1423
Mo(1)−S(1)	2.486(2)	2.5737
Mo(4)−S(2)	2.482 (2)	2.5735
Mo(2)−N(1)	2.187(4)	2.2204
Mo(3)−N(2)	2.208(4)	2.2202
C(1)−C(2)	1.500(7)	1.5167
C(1)−S(1)	1.740(6)	1.7712
C(2)−S(2)	1.737(5)	1.7712
C(1)−N(2)	1.308(6)	1.3218
C(2)−N(1)	1.315(6)	1.3212
Mo(1)−S(1)−C(1)	109.8(2)	102.961
Mo(4)−S(2)−C(2)	106.4(2)	102.968
Mo(2)−N(1)−C(2)	137.7(3)	132.519
Mo(3)−N(2)−C(1)	133.5(4)	132.525

shown below:

$$2Mo_2(DAniF)_3(O_2CCH_3) + CH_3(H)N(S)CC(S)N(H)CH_3 \xrightarrow[THF]{NaOCH_3} [Mo_2(DAniF)_3]_2(CH_3N(S)CC(S)NCH_3)$$

The ^{1}HNMR spectra (vide infra) are consistent with formation of a single product. Crystals were obtained by diffusion of isomeric hexanes into a solution of the product in CH_2Cl_2. The compound, shown in Figure 1, crystallized in the space group $P\bar{1}$ with the molecule residing on a general position. The crystallographically independent Mo−Mo bond distances of 2.0957(8) Å and 2.0898(8) Å (Table 1) are in the normal range for quadruple Mo−Mo bonds which have $\sigma^2\pi^4\delta^2$ electronic configurations.[17] The core has two six-membered rings, each composed of a dimolybdenum species and a S−C−C−N unit. The atom connectivity resembles that in the β form of the oxamidate analogues but unlike the oxamidate compounds there is a significant deviation from planarity in **1**, and the core resembles a butterfly. For comparison, the structural parameters for the core of an analogue that has the β form[16] and those in **1** are given in Scheme 2. For the dimethyloxamidate-linked compound, the torsion angles defined by N−C−C−N and O−C−C−O are 22.7° and 32.8°, respectively,[16] and there is a dihedral angle of 161° between the two Mo_2 axes. In general, for this type of compounds the torsion angles decrease as stepwise oxidation of the neutral compound takes place giving a planar heteronaphthalene-type structure for the doubly oxidized species.[10] For the sulfur derivative **1**, the torsion angles defined by N(1)−C(2)−C(1)−N(2) and S(1)−C(1)−C(2)−S(2) are 40.8° and 60.7°, respectively. These angles are considerably larger than those for the corresponding dimethyloxamidate-linked compound. The Mo−S−C and Mo−S−C angles are 109.8(2)° and 106.4(2)°, respectively. The butterfly structure is the result of the large difference in bond distances between Mo−S_{linker} (2.484[3] Å), C−S_{linker} (1.739[8] Å) and Mo−N_{linker} (2.198[7] Å), C−N_{linker} (1.312[9] Å), respectively. The corresponding Mo−O distances of 2.114(3) Å and 2.096(2) Å in the dimethyloxamidate analogue are about 0.38 Å shorter than the Mo−S distance in **1**. The average C−O distance is 1.290[5] Å, about 0.44 Å shorter than the average C−S distance. The distance of 6.409 Å between $[Mo_2]$ units in **1** is a little longer, 0.16 Å, than that of 6.248 Å in the dimethyloxamidate analogue.

In solution the molecule is fluxional as shown by the variable temperature ^{1}H NMR spectra. At room temperature there are two signals for the methine protons from the formamidinate groups (−NC*H*N−). One of them appears as a broad singlet at 8.35 ppm and the other one is sharp and

(17) (a) Lawton, D.; Mason, R. *J. Am. Chem. Soc.* **1965**, *87*, 921. (b) Cotton, F. A.; Mester, Z. C.; Webb, T. R. *Acta Crystallogr.* **1974**, *B30*, 2768. (c) Cotton, F. A.; Daniels, L. M.; Hillard, E. A.; Murillo, C. A. *Inorg. Chem.* **2002**, *41*, 1639.

Table 2. Electrochemical Data for **1** and Selected $[Mo_2](L)[Mo_2]$ Compounds[a]

compound	$Mo_2\cdots Mo_2$ (Å)	$E_{1/2}(+1/0)$[b] (mV)	$E_{1/2}(+2/+1)$[b] (mV)	$\Delta E_{1/2}$ (mV)	K_C[c]	ref.
$[(Bu^tCO_2)_3Mo_2]_2(O_2CC_6H_4CO_2)$	NA	0	NA	0	4	12
$[(Bu^tCO_2)_3Mo_2]_2$ $(OSCC_6H_4CSO)$	NA	0	184	184	1.3×10^3	12
oxamidate[d]	6.978	280	484	204	2.8×10^3	13
dithiooxamidate[d]	7.471	294	701	407	7.6×10^6	13
α-diphenyloxamidate[d]	7.096	176	367	191	1.7×10^3	10
β-diphenyloxamidate[d]	6.322	−157	383	540	1.3×10^9	10
β-dimethyloxamidate	6.248	−169	362	531	9.5×10^8	16
1	7.537	200	640	440	2.7×10^7	this work

[a] All potentials are referenced to Ag/AgCl. [b] $E_{1/2} = (E_{pa} + E_{pc})/2$ from the CV. [c] K_C is calculated using the formula $K_C = \exp(\Delta E_{1/2}/25.69)$. See ref 18b. [d] The dimetal units are $[Mo_2(DAniF)_3]^+$.

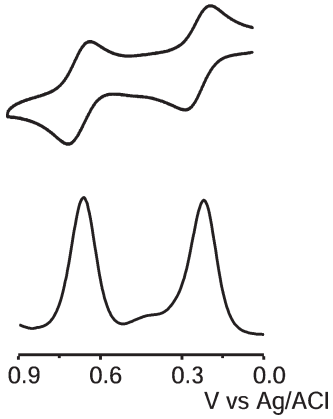

Figure 2. Cyclic voltammogram (with potentials vs Ag/AgCl) and differential pulse voltammogram for **1** in CH_2Cl_2 solution.

appears at 8.20 ppm. These are in a ratio of 4:2. At −50 °C these signals split into three sharp singlets in a ratio of 2:2:2 and appear at 8.54, 8.13, and 8.06 ppm. At room temperature the signals for the methoxy groups appear in a ratio of 12:12:6:6. The first set of signals correspond to the 12 hydrogen atoms for the *cis*-DAniF ligands on each side of the molecule, the other signals are for the corresponding groups in the *trans*-DAniF ligands. At −50 °C, all signals for the methoxy groups are independent. Similarly the signals for the aromatic protons also split (see Supporting Information). This is consistent with the wings of the molecule flipping back and forth, in the NMR time scale, in solution at room temperature but being essentially constrained at −50 °C to a structure similar to that in the solid state in which the distorted structure breaks the equivalence of the *cis*-DAniF ligands.

Electrochemical measurements generally provide useful information about the degree of the electronic interaction between redox centers.[18] The cyclovoltammogram (CV) and differential pulse voltammogram (DPV) for **1** are shown in Figure 2, and related electrochemical data are given in Table 2. The redox potentials ($E_{1/2}$) in CH_2Cl_2 for **1** are at 200 and 640 mV, with a $\Delta E_{1/2}$ of 440 mV. From this value, the comproportionation constant of 2.7×10^7 is calculated using the relationship $K_C = \exp(\Delta E_{1/2}/25.69)$.[19]

It should be noted that the $\Delta E_{1/2}$ for **1** is 91 mV smaller than that of the dimethyloxamidate analogue (531 mV) and K_C is almost 2 orders of magnitude smaller than that of the dimethyloxamidate compound (9.5×10^8).[16,20] Previously, we showed that by substitution of O-donor atoms in α-oxamidate linked compound to sulfur atoms there was an increase in the potential separation. This can be attributed not only to the lower orbital energy for the S-ligand than for the corresponding O-ligand but also to the availability of the 3d orbitals to the sulfur atom which may allow for multiple bond character. However, the situation is quite different for **1** than for the β form of the dimethyloxamidate-linked compound since the latter has a naphthalene-type structure that allows good π conjugation between the two fused six-membered rings. When an oxygen atom is replaced by a sulfur atom in this type of compound, the Mo−S and C−S distances are longer than the corresponding Mo−O and C−O distances, and more importantly by replacing O atoms by S atoms, the essentially planar conformation found in the oxidized oxamidate analogues does not exist in **1**. This hinders the conjugation pathway.

For more insight into the electronic structure of **1**, DFT calculations were performed using well developed methods for these systems.[10,13] Geometry optimization was performed on a model with H atoms instead of *p*-anisyl groups. These calculations satisfactorily reproduced the structural results and the highly distorted non-planar structure. Calculated bond distances and angles are shown in Table 1. The overestimation in bond distances is attributed to the lesser basicity of the H atoms relative to the *p*-anisyl groups.

In many of the previously reported calculations on *dimers of dimers*, the HOMO and HOMO-1 are composed of in-phase and out-of-phase combinations of the δ bonds because the two $[Mo_2]$ units are in the same plane and essentially parallel to each other.[21,22] Because of the distorted structure in **1** such interactions are unavailable as shown in Figure 3. It should be noted that the energy gap between the HOMO and HOMO-1 is generally used to evaluate the strength of the electronic coupling.[22] The calculated energy separation of 0.12 eV for **1** is significantly lower than that of 0.61 eV for the oxamidate analogue. Similar to the dithioxamidate linked compound,[13] the lowest unoccupied molecular orbital (LUMO) is the π* orbital from the linker. Time-dependent DFT (TD-DFT) calculations show that besides the δ to δ* transition (527 nm, $f = 0.0038$), there is a metal to ligand charge transfer transition (587 nm, $f = 0.0408$). Indeed, the UV−vis spectrum of **1** shows one intense absorption band at 460 nm and one at 580 nm (Figure 4), which are assigned to a

(18) (a) Cannon, R. D. *Electron-Transfer Reactions*; Butterworth: London, 1980. (b) Richardson, D. E.; Taube, H. *Inorg. Chem.* **1981**, *20*, 1278.
(19) Robin, M. B.; Day, P. *Adv. Inorg. Chem. Radiochem.* **1967**, *10*, 357.
(20) It should be noted that recently a report appeared of a pair containing a tetrathioterephthalate bridge. In this compound the distance between $[Mo_2]$ units is ca. 12 Å and the $\Delta E_{1/2}$ is only about half of that in **1**, namely, 250 mV. See: Han, M. J.; Liu, C. Y.; Tian, P. F. *Inorg. Chem.* **2009**, *48*, 6347.
(21) Cotton, F. A.; Li, Z.; Liu, C. Y.; Murillo, C. A.; Villagrán, D. *Inorg. Chem.* **2006**, *45*, 767.
(22) Cotton, F. A.; Murillo, C. A.; Villagrán, D.; Yu, R. *J. Am. Chem. Soc.* **2006**, *128*, 3281.

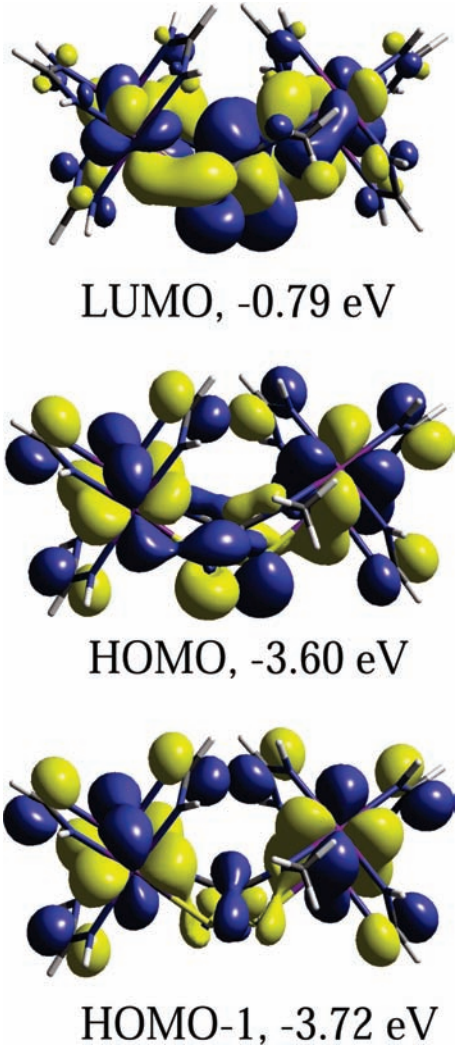

Figure 3. Illustration of the 0.02 contour surface diagrams for selected frontier orbitals in **1**.

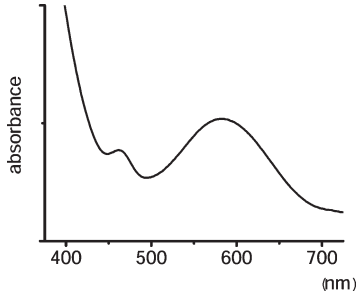

Figure 4. UV−vis spectrum of **1** in CH_2Cl_2 solution.

$\delta \rightarrow \delta^*$ transition and a MLCT band, respectively. In **1** two important opposing factors are in play. The low energy metal to ligand charge transfer can facilitate an electron-hopping pathway for the electron transfer and increase the electronic coupling.[12,13] However, the lack of an effective π system in **1** limits the pathway for effective electron delocalization. Evidently, the conjugation pathway plays a more important role than the electron hopping pathway in determining how the electronic communication is affected in this type of *dimers of dimers*.

Conclusions

In this work, the *dimer of dimers* containing two quadruply bonded $[Mo_2(DAniF)_3]^+$ units bridged by the S-donor linker, dimethyldithiooxamidate was synthesized. It has a core structure with two fused six-membered rings that show a substantial deviation from planarity. Electrochemical measurements show a $\Delta E_{1/2}$ of 440 mV which is much smaller than that of 531 mV for the O-donor analogue. This is different from what has been observed in previous studies that had shown that stepwise replacement of O to S from dicarboxylates[12] or replacing O-donor atoms in oxamidate to S-donor atoms[13] lead to enhancement in electronic coupling. This enhancement is due to dδ-dπ interactions between the dimetal units and the low-lying π^* orbital of the S atoms. It should be noted that for the dimethyloxamidate-linked compound there is a naphthalene-type structure, and good π conjugation in the two fused six-membered rings is possible. When O is replaced by S, the Mo−S and C−S distances are longer than the corresponding Mo−O and C−O distances, and more importantly by replacing O to S, the near planar conformation found in the oxidized oxamidate analogues does not exist in **1**, which blocks the conjugation pathway. DFT calculations show that the energy gap between HOMO and LUMO of 0.12 eV for **1** is much smaller than that of 0.61 eV for the O-donor analogue, which is consistent with the differences observed in the electrochemical studies. Comparison of **1** with that of the O-analogue clearly shows the importance of π conjugation in the O-analogue and the participation of δ bonds in such conjugation to modulate the electronic communication in many species containing *pairs of pairs* with quadruply bonded species.

Experimental Section

All reactions and manipulations were performed under a nitrogen atmosphere, using either a drybox or standard Schlenk line techniques. Solvents were purified under argon using a Glass Contour solvent purification system or distilled over appropriate drying agent under nitrogen. The starting materials, $Mo_2(DAniF)_3(O_2CCH_3)$[10a] and *N*,*N*′-dimethyldithiooxamide[23] were prepared according to reported procedures; other commercially available chemicals were used as received.

Physical and Characterization Measurements. Elemental analyses were performed by Robertson Microlit Laboratories, Madison, New Jersey. Electronic spectra were measured on a Shimadzu UV−2501PC spectrometer in CH_2Cl_2 solution. ^1H NMR spectra were recorded on a Inova−300 NMR spectrometer with chemical shifts (δ ppm) referenced to residual $CHCl_3$ in $CDCl_3$. Cyclic voltammograms and differential pulse voltammograms were collected on a CH Instruments electrochemical analyzer with Pt working and auxiliary electrodes, Ag/AgCl reference electrode, scan rate (for CV) of 100 mV/s, and 0.10 M $Bu^n_4NPF_6$ (in CH_2Cl_2) as electrolyte.

Preparation of $[Mo_2(DAniF)_3]_2(C_2S_2N_2Me_2)$, 1. To a solution of $Mo_2(DAniF)_3(OCCH_3)$ (406 mg, 0.400 mmol) and *N*,*N*′-dimethyldithiooxamide (29.5 mg, 0.200 mmol) in 25 mL of THF was added, slowly and with stirring, 0.80 mL of a sodium methoxide solution (0.5 M in CH_3OH). The reaction mixture was stirred at ambient temperature for 24 h, and the color turned from yellow to brownish blue. After removing the solvent under reduced pressure, the solid residue was extracted using CH_2Cl_2 (ca. 15 mL). The mixture was filtered using a Celite-packed frit,

(23) Hurd, R. N.; Delamater, G.; McElheny, G. C.; Wallingford, V. H.; Turner, R. J. *J. Org. Chem.* **1961**, *26*, 3980.

and the volume of the filtrate was reduced under vacuum to about 5 mL. Ethanol (40 mL) was then added to the solution producing a blue precipitate that was washed with ethanol (2 × 20 mL) and hexanes (20 mL). This solid was dried under vacuum, then dissolved in 15 mL of CH_2Cl_2 and layered with hexanes. Blue crystals formed within 7 days. Yield: 330 mg (80%). ^{1}H NMR ($CDCl_3$, δ in ppm). At 23 °C: 8.33 (s, 4H, −NC*H*N−), 8.20 (s, 2H, −NC*H*N−), 6.61 (d, 16H, aromatic C−*H*), 6.46 (d, 4H, aromatic C−*H*), 6.43 (d, 4H, aromatic C−*H*), 6.28 (d, 4H, aromatic C−*H*), 6.19 (d, 4H, aromatic C−*H*), 6.10 (d, 4H, aromatic C−*H*), 5.84 (d, 4H, aromatic C−*H*), 3.72 (s, 12H, −OCH_3), 3.71 (s, 12H, −OCH_3), 3.69 (s, 6H, −OCH_3), 3.58 (s, 6H, −OCH_3), 2.59 (s, 6H, −NCH_3). At −50 °C: 8.54 (s, 2H, −NC*H*N−), 8.13 (s, 2H, −NC*H*N−), 8.06 (s, 2H, −NC*H*N−), 6.38−6.68 (m, 24H, aromatic C−*H*), 6.27 (d, 4H, aromatic C−*H*), 6.18 (d, 4H, aromatic C−*H*), 6.10 (d, 4H, aromatic C−*H*), 5.80 (d, 4H, aromatic C−*H*), 3.76 (s, 6H, −OCH_3), 3.74 (s, 6H, −OCH_3), 3.70 (s, 6H, −OCH_3), 3.69 (s, 6H, −OCH_3), 3.66 (s, 6H, −OCH_3), 3.58 (s, 6H, −OCH_3), 2.54 (s, 6H, −NCH_3). UV−vis, λ_{max} nm (ε, $M^{-1}\cdot mol^{-1}$): 580 (8.0 × 10^3), 460 (1.6 × 10^3). Anal. Calcd. for $C_{94}H_{96}Mo_4N_{14}O_{12}S_2$: C, 54.76; H, 4.69; N, 9.51. Found: C, 54.48; H, 4.47; N, 9.31.

X-ray Crystallography. Single crystals were obtained by diffusion of hexanes to a dichloromethane solution of **1**. Data were collected on a Bruker SMART 1000 CCD area detector system. Cell parameters were determined using the program SMART.[24] Data reduction and integration were performed with the software SAINT.[25] Absorption corrections were applied by using the program SADABS.[26] The positions of the Mo atoms were found via direct methods using the program SHELXTL.[27] Subsequent cycles of least-squares refinement followed by difference Fourier syntheses revealed the positions of the remaining non-hydrogen atoms. Hydrogen atoms were added in idealized positions. All non-hydrogen atoms were refined with anisotropic displacement parameters. The solvent dichloromethane molecules were disordered and refined with suitable constrains. Selected bond distances and angles are listed in Table 1 and crystallographic data are given in Table 3.

Computational Calculations. DFT[28] calculations were performed with the hybrid Becke's[29] three-parameter exchange functional and the Lee−Yang−Parr[30] nonlocal correlation functional (B3LYP) in the Gaussian 03 program.[31] Double-ζ quality basis sets (D95)[32] were used on C, N, and H atoms as implemented in Gaussian. For O and S atoms, correlation consistent double-ζ basis sets (CC−PVDZ)[33] were applied. A small effective core potential (ECP) representing the 1s2s2p3s3p3d core was used for the molybdenum atoms along with its corresponding double-ζ basis set (LANL2DZ).[34] Time-dependent density functional (TD−DFT) calculations[35] were used for the assignment of the electronic spectra. All calculations were performed using Origin 3800 64−processor SGI or Origin 2000 32−processor SGI supercomputers located at the Texas A&M supercomputing facility.

Table 3. X-ray Crystallographic Data for **1**·1.5CH_2Cl_2

	1·1.5CH_2Cl_2
empirical formula	$C_{95.5}H_{98}Cl_3S_2Mo_4N_{14}O_{12}$
fw	2188.11
space group	$P\bar{1}$ (No. 2)
a, Å	14.757(3)
b, Å	17.823(4)
c, Å	20.360(5)
α, deg	73.391(4)
β, deg	88.599(4)
γ, deg	68.105(4)
V, Å^3	4741.0(19)
Z	2
T, K	213
λ, Å	0.71073
d_{calcd}, g/cm^3	1.563
μ, mm^{-1}	0.714
R1[a] (wR2[b])	0.0885 (0.1491)

[a] $R1 = \sum||F_o| - |F_c||/\sum|F_o|$. [b] $wR2 = [\sum w(F_o^2 - F_c^2)^2/\sum w(F_o^2)^2]^{1/2}$.

Acknowledgment. We thank the Robert A. Welch Foundation and Texas A&M University for financial support and Gina M. Chiarella for help in the final crystallographic refinement. C.A.M. also thanks the National Science Foundation (IR/D support).

Supporting Information Available: X-ray crystallographic data for **1**·2CH_2Cl_2 in standard CIF format. ^{1}H NMR spectra in pdf for **1** in $CDCl_3$ solution at 23 and −50 °C. This material is available free of charge via the Internet at http://pubs.acs.org.

(24) *SMART for Windows NT*, version 5.618; Bruker Advanced X-ray Solutions, Inc.: Madison, WI, 2001.
(25) *SAINT, Data Reduction Software*., version 6.36A; Bruker Advanced X-ray Solutions, Inc.: Madison, WI, 2001.
(26) *SADABS, Area Detector Absorption and other Corrections Software*, version 2.05; Bruker Advanced X-ray Solutions, Inc.: Madison, WI, 2001.
(27) Sheldrick, G. M. *SHELXTL*, version 6.12; Bruker Advanced X-ray Solutions, Inc.: Madison, WI, 2002.
(28) (a) Hohenberg, P.; Kohn, W. *Phys. Rev.* **1964**, *136*, B864. (b) Parr, R. G.; Yang, W. *Density−Functional Theory of Atoms and Molecules*, Oxford University Press: Oxford, 1989.
(29) (a) Becke, A. D. *Phys. Rev. A* **1988**, *38*, 3098. (b) Becke, A. D. *J. Chem. Phys.* **1993**, *98*, 1372. (c) Becke, A. D. *J. Chem. Phys.* **1993**, *98*, 5648.
(30) Lee, C. T.; Yang, W. T.; Parr, R. G. *Phys. Rev. B* **1998**, *37*, 785.
(31) Frisch, M. J.; Trucks, G. W.; Schlegel, H. B.; Scuseria, G. E.; Robb, M. A.; Cheeseman, J. R.; Montgomery, Jr., J. A.; Vreven, T.; Kudin, K. N.; Burant, J. C.; Millam, J. M.; Iyengar, S. S.; Tomasi, J.; Barone, V.; Mennucci, B.; Cossi, M.; Scalmani, G.; Rega, N.; Petersson, G. A.; Nakatsuji, H.; Hada, M.; Ehara, M.; Toyota, K.; Fukuda, R.; Hasegawa, J.; Ishida, M.; Nakajima, T.; Honda, Y.; Kitao, O.; Nakai, H.; Klene, M.; Li, X.; Knox, J. E.; Hratchian, H. P.; Cross, J. B.; Bakken, V.; Adamo, C.; Jaramillo, J.; Gomperts, R.; Stratmann, R. E.; Yazyev, O.; Austin, A. J.; Cammi, R.; Pomelli, C.; Ochterski, J. W.; Ayala, P. Y.; Morokuma, K.; Voth, G. A.; Salvador, P.; Dannenberg, J. J.; Zakrzewski, V. G.; Dapprich, S.; Daniels, A. D.; Strain, M. C.; Farkas, O.; Malick, D. K.; Rabuck, A. D.; Raghavachari, K.; Foresman, J. B.; Ortiz, J. V.; Cui, Q.; Baboul, A. G.; Clifford, S.; Cioslowski, J.; Stefanov, B. B.; Liu, G.; Liashenko, A.; Piskorz, P.; Komaromi, I.; Martin, R. L.; Fox, D. J.; Keith, T.; Al−Laham, M. A.; Peng, C. Y.; Nanayakkara, A.; Challacombe, M.; Gill, P. M. W.; Johnson, B.; Chen, W.; Wong, M. W.; Gonzalez, C.; and Pople, J. A. *Gaussian 03*, revision C.02; Gaussian, Inc.: Wallingford, CT, 2004.
(32) (a) Dunning, T. H.; Hay, P. J. In *Modern Theoretical Chemistry*. *3. Methods of Electronic Structure Theory*; Schaefer, H. F., III, Ed.; Plenum Press: New York, 1977; pp.1−28. (b) Woon, D. E.; Dunning, T. H. *J. Chem. Phys.* **1993**, *98*, 1358.
(33) (a) Dunning, T. H. *J. Chem. Phys.* **1989**, *90*, 1007. (b) Woon, D. E.; Dunning, T. H. *J. Chem. Phys.* **1993**, *98*, 1358. (c) Wilson, A. K.; Woon, D. E.; Peterson, K. A.; Dunning, T. H. *J. Chem. Phys.* **1999**, *110*, 7667.
(34) (a) Wadt, W. R.; Hay, P. J. *J. Chem. Phys.* **1985**, *82*, 284. (b) Hay, P. J.; Wadt, W. R. *J. Chem. Phys.* **1985**, *82*, 299.
(35) Casida, M. E.; Jamorski, C.; Casida, K. C.; Salahub, D. R. *J. Chem. Phys.* **1998**, *108*, 4439.